JOURNAL OF VIROLOGY, Sept. 2006, p. 8763–8777 Vol. 80, No. 17
0022-538X/06/$08.00+0 doi:10.1128/JVI.00598-06

Interaction between Vaccinia Virus Extracellular Virus Envelope A33 and B5 Glycoproteins

Beatriz Perdiguero† and Rafael Blasco*

Departamento de Biotecnología, INIA, Ctra. La Coruña km 7.5, 28040 Madrid, Spain

Received 24 March 2006/Accepted 15 June 2006

The extracellular form of vaccinia virus acquires its outer envelope by wrapping with cytoplasmic membranes that contain at least seven virus-encoded proteins, of which four are glycoproteins. We searched for interactions between the vaccinia virus A33 glycoprotein and proteins A34, A36, B5, F12, and F13. First, when *myc* epitope-tagged A33 was expressed in combination with other envelope proteins, A33 colocalized with B5 and A36, suggesting that direct A33-B5 and A33-A36 interactions occur in the absence of infection. A recombinant vaccinia virus (vA33R*myc*) was constructed by introduction of the *myc*-tagged A33 version (A33*myc*) into A33-deficient vaccinia virus. A33*myc* partially restored plaque formation and colocalized with enveloped virions in infected cells. Coimmunoprecipitation experiments with extracts of vA33R*myc*-infected cells confirmed the existence of a physical association of A33 with A36 and B5. Of these, the A33-B5 interaction is a novel finding, whereas the interaction between A33 and A36 has been previously characterized. A collection of vaccinia viruses expressing mutated versions of the B5 protein was used to investigate the domain(s) of B5 required for interaction with A33. Both the cytoplasmic domain and most of the extracellular domain, but not the transmembrane domain, of the B5 protein were dispensable for binding to A33. Mutations in the extracellular portions of B5 and A33 that enhance extracellular virus release did not affect the interaction between the two. In contrast, substituting the B5 transmembrane domain with that of the vesicular stomatitis virus G glycoprotein prevented the association with A33. Immunofluorescence experiments on virus mutants indicated that B5 is required for efficient targeting of A33 into enveloped virions. These results point to the transmembrane domain of B5 as the major determinant of the A33-B5 interaction and demonstrate that protein-protein interactions are crucial in determining the composition of the virus envelope.

Vaccinia virus is the most studied member of the family *Poxviridae*, which includes structurally large and genetically complex DNA viruses that replicate and assemble in the cytoplasm of infected cells. Vaccinia virus particles are assembled and released through different stages, including those of the noninfectious immature virus (IV), the intracellular mature virus (IMV), the intracellular enveloped virus (IEV), the cell-associated enveloped virus (CEV), and the extracellular enveloped virus (EEV) (24, 36, 37). IMV particles are cytosolic and remain intracellular until the cells are lysed. Some IMVs leave the assembly areas in a microtubule-dependent movement and become wrapped by a double layer of intracellular membranes derived from the early endosomes (38, 39) or *trans*-Golgi network (34) to form IEV. Subsequently, IEVs move to the cell surface (again requiring microtubules), where the outer membrane fuses with the plasma membrane, thus generating enveloped virions, with an extra membrane with respect to IMV, at the cell surface. Particles that remain attached to the plasma membrane are termed CEV, while those released are called EEV (2). In cell culture, enveloped virions (CEV plus EEV) are responsible for virus transmission, since mutants that form normal amounts of IMV but are blocked in virus wrapping are impaired in transmission (1). Specific roles in virus transmission have been assigned to CEV and EEV. CEV particles can induce the formation of actin tails, which are important for efficient cell-to-cell spread. Conversely, EEVs mediate long-range dissemination of virus (2, 6, 28).

Seven virus-encoded IEV envelope proteins have been described and characterized. The A33 (29), A34 (7), B5 (9, 16), F13 (14), and A56 (35) proteins are present in IEV, CEV, and EEV, although approximately one-third of EEV particles lack A56 (20). Proteins A36 and F12 are present in IEV but absent from CEV and EEV envelopes (26, 39, 40, 46). The proteins present in the IEV and EEV envelopes have been shown to have different roles in the morphogenetic pathway. For instance, proteins B5 and F13 are required for efficient and complete wrapping of IMV. Proteins A36 and F12 are involved in the microtubule-mediated transport of IEV to the cell surface. Actin tail formation requires the A33, A34, A36, and B5 proteins. Finally, release of CEV to form EEV is modulated by mutations in the A33, A34, and B5 proteins (4, 12, 17, 18).

Vaccinia IEV envelope proteins must be incorporated and retained in the wrapping membranes to allow proper assembly of progeny viruses, and these events are probably mediated by protein-protein interactions involving viral and cellular proteins. To date, A33-A36, A34-B5, A34-A36 (31), B5-F13 (27), A36-Nck (10), and A36-Grb2 (33) interactions have been described. It is likely that identifying the protein interactions between envelope proteins will help us to understand the mechanisms mediating events such as IMV and IEV transport or IMV wrapping. Our present work focuses on the identification of interactions between A33 and the rest of the IEV

* Corresponding author. Mailing address: Dpto. Biotecnología, INIA, Ctra. La Coruña km 7.5, 28040 Madrid, Spain. Phone: 34-91-347 39 13. Fax: 34-91-357 22 93. E-mail: blasco@inia.es.

† Present address: Departamento de Biología Molecular y Celular, Centro Nacional de Biotecnología, CSIC, Campus Universidad Autónoma, 28049 Madrid, Spain.

envelope proteins and their functional implications in the morphogenetic pathway.

MATERIALS AND METHODS

Cells and viruses. BSC-1 and CV-1 cells were grown in minimal essential medium supplemented with 5% fetal bovine serum (FBS). BHK-21 cells (ATCC CCL10) were grown in BHK Glasgow minimal essential medium containing 5% FBS, 3 g/ml tryptose phosphate broth, and 0.01 M HEPES. Virus infections were performed with 2% FBS for all cell types. Vaccinia viruses vΔB5R (44) and vΔA33R (30) were made available by B. Moss.

Antibodies. Mouse monoclonal antibody VMC-34 (anti-A33) was provided by G. H. Cohen. Anti-A36 mouse monoclonal antibody was made available by G. L. Smith. Rat monoclonal antibodies 19C2 (anti-B5) and 15B6 (anti-F13) were kindly made available by G. Hiller. Mouse monoclonal antibodies 4C5/CR3 (anti-porcine antigen) and 3B11/11 (anti-porcine sialoadhesin) were provided by C. Revilla and B. Álvarez and were used as control immunoglobulin G (IgG) in coimmunoprecipitation experiments.

Plasmid construction. The coding sequence of the A33R gene was amplified by PCR, using the genome of vaccinia virus strain Western Reserve (WR) as the template and oligonucleotide primers A33R-E (5′-CATTGAATTCCATGATG ACACCAG-3′) (EcoRI site underlined) and A33R-X (5′-AAATTCTAGATA GTTCATTGTTTTAAC-3′) (XbaI site underlined). The PCR product was digested with EcoRI and XbaI and inserted into EcoRI/XbaI-digested pcDNA 3.1/*myc*-HisB (Invitrogen) to generate pcDNA 3.1/*myc*-HisB-A33R. Primer A33R-X eliminated the stop codon at the end of the A33R gene and provided in-frame fusion with the *myc*His_6 epitope.

To generate plasmid pcDNA 3.1/HA-HisB, the influenza virus hemagglutinin (HA) epitope was obtained by annealing of oligonucleotide primers HA-X (5′-CTAGAGTACCCATATGATGTTCCAGATTATGCTTAAA-3′) and HA-A (5′-CCGGTTTAAGCATAATCTGGAACATCATATGGGTACT-3′). The HA epitope was inserted into plasmid pcDNA 3.1/*myc*-HisB previously digested with XbaI and AgeI to eliminate the *myc* epitope. Primer HA-X inserted a stop codon at the end of the HA epitope.

The coding sequence of the A34R gene was amplified by PCR, using plasmid pSFV-A34R (21) as the template and oligonucleotide primers A34R-E (5′-GT ACATGAATTCATGAAATCGCTTAATAG-3′) (EcoRI site underlined) and A34R-X (5′-CATTTTTTCTAGAGACTTGTAGAATT-3′) (XbaI site underlined). The PCR product was cut with EcoRI and XbaI and inserted into EcoRI/XbaI-digested pcDNA 3.1/HA-HisB to generate pcDNA 3.1/HA-HisB-A34R. Primer A34R-X eliminated the stop codon at the end of the A34R gene and provided in-frame fusion with the influenza virus HA epitope.

The coding sequence of the A36R gene was amplified by PCR, using the WR genome as the template and oligonucleotide primers A36R-N (5′-ATTGAGCT AGCAGAAATGATGCTGGTA-3′) (NheI site underlined) and A36R-B (5′-T AAAAAGGATCCTAATCACACCAATG-3′) (BamHI site underlined). The PCR product was cut with NheI and BamHI and inserted into NheI/BamHI-digested pcDNA 3.1(+) (Invitrogen) to generate pcDNA 3.1/A36R.

The B5R gene was obtained by digestion of plasmid pSFV-B5R (21) with SmaI and subcloning into plasmid pSG5 (Stratagene) previously digested with BamHI and treated with a Klenow fragment of *Escherichia coli* DNA polymerase I. The resulting plasmid was termed pSG5-B5R.

The coding sequence of the F12L gene was amplified by PCR, using the WR genome as the template and oligonucleotide primers F12L-SacII (5′-CCCCCG CGGATGTTAAACAGGGTACAA-3′) (SacII site underlined) and F12L-NheI (5′-CCCGCTAGCGTTTAATTTTACCATCTG-3′) (NheI site underlined). The PCR product was cut with SacII and NheI and inserted into SacII/NheI-digested pQBI-25 (CPG, Inc.), encoding the rsGFP protein, to generate pQBI-F12L. Primer F12L-NheI eliminated the stop codon at the end of the F12L gene and provided in-frame fusion with the rsGFP gene.

The coding sequence of the F13L gene fused to the rsGFP gene was amplified by PCR, using plasmid pRB-p37g-*pac* as the template and oligonucleotide primers P37-H (5′-TTATGTTAAGCTTATGTGGCCATTTGCATCG-3′) (HindIII site underlined) and rsGFP-B (5′-TACTAGTGGATCCTCAGTTGTACAGTT C-3′) (BamHI site underlined). The PCR product was cut with HindIII and BamHI and inserted into plasmid pcDNA 3.1(+) previously digested with the same restriction enzymes to generate pcDNA 3.1/p37g. Plasmid pRB-p37g-*pac*, used as the template, was obtained as follows. The coding sequence of the end of the F13L gene fused to the rsGFP gene was amplified by PCR, using the W-P37g (11) genome as the template and oligonucleotide primers A328Gf (5′-TCATATCACTTCGGGAAATTTCGACGG-3′) and GFP H3 (5′-TTTACTA GTGAAGCTTCCGTTGTACAG-3′) (HindIII site underlined). The PCR product was cut with AflII and HindIII and inserted into AflII/HindIII-digested pRB-GFP-*pac* (32).

Plasmid pGem-A33Rmg, used for the construction of a recombinant vaccinia virus expressing a *myc*His_6 epitope fused to the C terminus of the A33 protein (vA33R*myc*), was obtained by the sequential cloning of four DNA fragments containing the rsGFP gene, *myc*His_6 epitope, A33R gene, and A33R recombination flanking sequences into plasmid pGem-7Zf(−) (Promega). The rsGFP gene under the control of the vaccinia virus synthetic early/late promoter was amplified by PCR from plasmid pGem-*pac*-rsGFP (obtained by the cloning of rsGFP and puromycin acetyltransferase [*pac*] genes into pGem-7Zf) with oligonucleotides rsGFP-Nsi (5′-GCCTGACGCATGCATGAGAAAAATTG-3′) (NsiI site underlined) and Sp6 (5′-ATTTAGGTGACACTATAGAA-3′). The PCR product was cut with NsiI and inserted into NsiI-digested pGem-7Zf(−) to generate pGem-rsGFP. The *myc*His_6 epitope was amplified by PCR from plasmid pcDNA 3.1/*myc*-HisB with oligonucleotides *myc*-X (5′-GCACAGTGGCG GCCGCTCGAGTCTAGAGG-3′) (XbaI site underlined) and *myc*-E (5′-GAG GCTGATCAGCGGAATTCAACTCAATG-3′) (EcoRI site underlined). The PCR product was digested with XbaI and EcoRI. The left flank and coding sequence of the A33R gene were amplified by PCR from the WR genome with oligonucleotides A33R-S (5′-CAAGAATGCATGCTTATATTTTTTAACTA G-3′) (SphI site underlined) and A33R-X (5′-AAATTCTAGATAGTTCATTG TTTTAAC-3′) (XbaI site underlined). The PCR product was digested with SphI and XbaI. Primer A33R-X eliminated the stop codon at the end of the A33R gene and provided in-frame fusion with the *myc*His_6 epitope. Finally, the WR genome was used as the template to amplify the right flank of the A33R gene with oligonucleotides fd33-E (5′-AAAAGAATTCGACTAATATTTATTTTT G-3′) (EcoRI site underlined) and A33Rfd-B (5′-ATTAGGATCCAACCATT TATCATTGG-3′) (BamHI site underlined). The PCR product was cut with EcoRI and BamHI.

Plasmid pG-B5R-V5-Red2, used for the construction of recombinant viruses WRΔB5R and vA33R*myc*ΔB5R, in which 94% of the B5R coding sequence has been replaced with a dsRed2 expression cassette, was obtained by the sequential cloning of four DNA fragments containing the dsRed2 gene, B5R recombination flanking sequences, and V5 epitope into the previously described pGem-rsGFP plasmid. The dsRed2 gene under the control of the synthetic early/late promoter was amplified by PCR from plasmid pRB-dsRed2 (encoding the products of the F13L and dsRed2 genes between the F13L flanking regions) with oligonucleotides Red2-X (5′-GTCTTTCTAGATAACTCGAGAAAA-3′) (XbaI site underlined) and Red2-E (5′-GATCCAGAATTCTATTTTATTTAGG-3′) (EcoRI site underlined). The PCR product was cut with XbaI and EcoRI. The WR genome was used as the template to amplify the right flank of the B5R gene with oligonucleotides fdB5R-E (5′-GCTAGAATTCATATAAATCCGTTAA-3′) (EcoRI site underlined) and fdB5R-B (5′-AGTATTCCGGGATCCACGCTTA CAG-3′) (BamHI site underlined). The PCR was digested with EcoRI and BamHI. The left flank and signal peptide sequences of the B5R gene were amplified by PCR from the WR genome with oligonucleotides fiB5R-S (5′-CA AAGGCATGCATACTTTAATGAG-3′) (SphI site underlined) and fiB5R-X (5′-CAGTTCTAGATGAATAAACAACAGC-3′) (XbaI site underlined). The PCR product was cut with SphI and XbaI. Finally, the V5 epitope was obtained by the annealing of oligonucleotides V5-Fc (5′-CTAGCGGTAAGCCTATCCC TAACCCTCTCCTCGGTCTCGATTCTACGT-3′) and V5-Rc (5′-CTGAGTA GAATCGAGACCGAGGAGAGGGTTAGGGATAGGCTTACCG-3′) and was inserted into the plasmid previously digested with XbaI.

For the construction of the recombinant viruses expressing different mutated versions of V5-tagged B5 protein, eight mutated versions of the B5R gene, schematically depicted in Fig. 5, were inserted into the B5R locus of virus mutant WRΔB5R, in which the B5R coding sequence is replaced by a dsRed expression cassette. These mutated versions without signal peptide sequences were amplified by PCR and inserted separately into the previously described pG-B5R-V5-Red2 plasmid digested with XbaI and EcoRI to generate plasmids pG-V5-B5Ra to pG-V5-B5Rf.

Version RSTC. The B5R gene was amplified by PCR from the WR genome with oligonucleotides B5R-Xa (5′-GTTTCTAGAACATGTACTGTACCC-3′) (XbaI site underlined) and B5R-Ma (5′-CGGATCAATTGTTACGGTAGCAA T-3′) (MunI site underlined). The PCR product was cut with XbaI and MunI and inserted into plasmid pG-B5R-V5-Red2 to generate plasmid pG-V5-B5Ra.

Version RST. The B5R gene without the sequence for the cytoplasmic tail was amplified by PCR from the WR genome with oligonucleotides B5R-Xa (5′-GT TTCTAGAACATGTACTGTACCC-3′) (XbaI site underlined) and B5R-Mb (5′-ATTGCAATTGTTATTTGTCACAGG-3′) (MunI site underlined). Primer B5R-Mb inserted a stop codon at the end of B5R version RST. The PCR product was cut with XbaI and MunI and inserted into plasmid pG-B5R-V5-Red2 to generate plasmid pG-V5-B5Rb.

Version TC. The sequences corresponding to the transmembrane and cytoplasmic domains of the B5 protein were amplified by PCR from plasmid pG-V5-B5Ra with oligonucleotides B5R-Xc (5′-GAAATATCTAGATTAGAAGCAAC-3′) (XbaI site underlined) and B5R-Ec (5′-ATATGAATTCTTACGGTAGCAA-3′) (EcoRI site underlined). The PCR product was cut with XbaI and EcoRI and inserted into plasmid pG-B5R-V5-Red2. The resulting plasmid was termed pG-V5-B5Rc.

Version STC. The sequences of the stalk, transmembrane, and cytoplasmic domains of the B5 protein were amplified by PCR from plasmid pG-V5-B5Ra with oligonucleotides B5R-Xc+49 (5′-CATCATCTAGATGTATCGACGG-3′) (XbaI site underlined) and B5R-Ec (5′-ATATGAATTCTTACGGTAGCAA-3′) (EcoRI site underlined). The PCR product was cut with XbaI and EcoRI and inserted into plasmid pG-B5R-V5-Red2 to generate plasmid pG-V5-B5Rc+49.

Version RS. The sequence for the extracellular domain of the B5 protein was amplified by PCR from the WR genome with oligonucleotides B5R-Xa (5′-GTTTCTAGAACATGTACTGTACCC-3′) (XbaI site underlined) and B5R-Md (5′-TATGCAATTGTTATTCTAACGATTC-3′) (MunI site underlined). Primer B5R-Md inserted a stop codon at the end of B5R version RS. The PCR product was cut with XbaI and MunI and inserted into pG-B5R-V5-Red2. The resulting plasmid was termed pG-V5-B5Rd.

Version R. The sequence for the four short consensus repeats (SCRs) of the B5 protein was amplified by PCR from the WR genome with oligonucleotides B5R-Xa (5′-GTTTCTAGAACATGTACTGTACCC-3′) (XbaI site underlined) and B5R-Md-51 (5′-TTACCCAATTGTTATGTGGATGATG-3′) (MunI site underlined). Primer B5R-Md-51 inserted a stop codon at the end of B5R version R. The PCR product was digested with XbaI and MunI and inserted into plasmid pG-B5R-V5-Red2 to generate plasmid pG-V5-B5Rd-51.

Version RST$_G$C. The sequence for the transmembrane domain of the vesicular stomatitis virus (VSV) G protein was amplified by PCR from G protein cloned in plasmid pRB-G-AR with oligonucleotides G1 (5′-GGACCAGTTCAGGATATAAGTTTCC-3′) and G2 (5′-CATTATTTTTGTCGAGAACCAAGAATAG-3′). The sequence for the cytoplasmic tail of the B5 protein was amplified by PCR from plasmid pG-V5-B5Ra with oligonucleotides B1 (5′-GACAAAAATAATGACCAATATAAG-3′) and B2 (5′-GTACTATATCATCGAACGGTATAAC-3′). Overlapping ends were included in oligonucleotides G2 and B1 to allow the annealing of the two PCR products (the underlined overlapping regions correspond to the initial sequence for the cytoplasmic tail of the B5 protein). By recombinant PCR, using these two PCR products as templates and inner oligonucleotides GB-X (5′-GGAAATCTAGAATTGCCTCTTTTTTC-3′) (XbaI site underlined) and B5R-Ec (5′-ATATGAATTCTTACGGTAGCAA-3′) (EcoRI site underlined), a DNA fragment with the sequence for the transmembrane domain of the G protein fused to the sequence for the cytoplasmic tail of the B5 protein was obtained. The resulting PCR product was cut with XbaI and EcoRI and inserted into plasmid pG-B5R-V5-Red2 to generate pG-V5-B5Re1. The sequence for the extracellular domain of the B5 protein was amplified by PCR from plasmid pG-V5-B5Ra with oligonucleotides B5R-Xa (5′-GTTTCTAGAACATGTACTGTACCC-3′) (XbaI site underlined) and B5R-Xe2 (5′-GATATCTAGATTCTAACGATTC-3′) (XbaI site underlined). The PCR product was digested with XbaI and inserted into plasmid pG-V5-B5Re1 to generate pG-V5-B5Re2, which encodes a B5 protein with the transmembrane domain replaced with that of the G protein.

Version R*STC. A B5 protein with a P189S mutation was constructed using a QuikChange XL site-directed mutagenesis kit (Stratagene). Plasmid pG-V5-B5Ra was used as the template, and a P189S mutation was inserted with oligonucleotides B5Rf-1 (5′-CAACAAAAATGTGATATGTCGTCTCTATCTAATGG-3′) and B5Rf-2 (5′-CCATTAGATAGAGACGACATATCACATTTTTGTTG-3′). The underlined nucleotides were used to introduce the P189S mutation.

Construction of recombinant viruses. Virus recombinants were isolated following infection/transfection experiments. Plasmids were transfected by use of Fugene transfection reagent (Roche), following the manufacturer's recommendations. vA33R*myc* was constructed by transient dominant selection, using the rsGFP gene as the transiently selectable marker. CV-1 cells were infected with vΔA33R at 0.05 PFU per cell and transfected 1 h later with pGem-A33Rmg. vA33R*myc* was isolated from progeny virus by rounds of plaque purification on BSC-1 cells (8), during which the plaques were screened for green fluorescent protein (GFP) fluorescence and plaque size (3). WRΔB5R and vA33R*myc*ΔB5R were also constructed by transient dominant selection, using the rsGFP gene as the selectable marker. CV-1 cells were infected with WR or vA33R*myc* at 0.05 PFU per cell and transfected 1 h later with pG-B5R-V5-Red2. WRΔB5R and vA33R*myc*ΔB5R were isolated from progeny virus by rounds of plaque purification on CV-1 cells stably expressing the B5 protein (Perdiguero and Blasco, unpublished), during which the plaques were screened for GFP/dsRed2 fluorescence. Recombinant viruses expressing different mutated versions of the B5 protein tagged with the V5 epitope were constructed by transient dominant selection using the rsGFP gene as the selectable marker. CV-1 cells were infected with WRΔB5R at 0.05 PFU per cell and transfected 1 h later with pG-V5-B5Ra to pG-V5-B5Rf. Recombinants were isolated from progeny virus by rounds of plaque purification on BSC-1 cells, during which the plaques were screened for GFP/dsRed2 fluorescence.

Immunofluorescence microscopy. BHK-21 cells grown to 70% confluence on round coverslips were infected with vaccinia virus at five PFU per cell or transfected with 1 μg of total plasmid DNA (500 ng of each plasmid in cotransfection experiments), using Fugene as the transfectant agent. At 7 h postinfection or 24 h posttransfection, the cells were washed with phosphate-buffered saline (PBS), fixed for 15 min at room temperature with cold 4% paraformaldehyde, and then washed with PBS and permeabilized by incubation for 15 min with PBS–0.1% Triton X-100. After being washed with PBS, the cells were incubated for 5 min with PBS containing 0.1 M glycine and then with primary antibody diluted in PBS-20% FBS (1:200 for anti-*myc* [Invitrogen], 1:20 for anti-HA-fluorescein [Roche], 1:50 for anti-*myc*-fluorescein isothiocyanate [FITC; Invitrogen], 1:200 for anti-V5 [Invitrogen], 1:50 for anti-A36, 1:100 for anti-B5, and 1:50 for anti-F13) for 30 min. After being washed with PBS, the cells were incubated for 30 min with secondary antibody diluted in PBS-20% FBS (1:200 for rabbit anti-mouse IgG-tetramethyl rhodamine isocyanate [TRITC; DAKO]). Some preparations were also incubated with 2 mg/ml bisbenzimide Hoechst or 1 unit/ml Alexa594-phalloidin (Molecular Probes) for 30 min at room temperature. Finally, the cells were extensively washed with PBS, mounted with FluorSave reagent (Calbiochem), and observed by fluorescence microscopy.

Western blotting. Western blots of infected cell lysates were made using BSC-1 cells grown in six-well plates and harvested at 24 h postinfection in denaturant buffer (80 mM Tris-HCl [pH 6.8], 2% sodium dodecyl sulfate [SDS], 10% glycerol, and 0.01% bromophenol blue solution, with or without 0.71 M 2-mercaptoethanol). Proteins were resolved by electrophoresis in 12% SDS-polyacrylamide gels. After SDS-polyacrylamide gel electrophoresis (PAGE), separated proteins were transferred to nitrocellulose. Membranes were incubated overnight at 4°C with primary antibody diluted in PBS containing 0.05% Tween 20 and 1% nonfat dry milk (1:50 for anti-F13). After being washed with PBS-0.05% Tween 20, the membranes were incubated for 1 h at room temperature with goat anti-rat IgG (diluted 1:3,000 in PBS-0.05% Tween 20-1% nonfat dry milk) conjugated with horseradish peroxidase (HRP; Amersham). After extensive washing with PBS-0.05% Tween 20, the membranes were incubated for 1 min with a 1:1 mixture of solution A (2.5 mM luminol [Sigma], 0.4 mM *p*-coumaric acid [Sigma], 100 mM Tris-HCl [pH 8.5]) and solution B (0.018% H_2O_2, 100 mM Tris-HCl [pH 8.5]) and exposed to X-ray film. Primary antibodies conjugated with horseradish peroxidase were also used (1:1,000 for anti-*myc*-HRP [Roche] and 1:5,000 for anti-V5-HRP [Invitrogen]).

Immunoprecipitation. BSC-1 cells (7.5×10^6) were infected with vaccinia virus at five PFU per cell. At 24 h postinfection, the cells were lysed with NP-40 lysis buffer (1% NP-40, 50 mM Tris-HCl [pH 7.6], 150 mM NaCl, 2 mM EDTA) or digitonin lysis buffer (1% digitonin [Sigma], 10 mM triethanolamine [pH 7.8; Merck], 150 mM NaCl, 1 mM EDTA), with 10 mM phenylmethylsulfonyl fluoride (Boehringer Mannheim) as the protease inhibitor, for 30 min at 4°C. The lysed cells were scraped and spun down for 20 min at 13,000 rpm and 4°C. The supernatant was harvested and precleared by incubation with protein G-Sepharose beads (Amersham) for 1 h at 4°C in a tube rotator. After centrifugation for 1 min at 13,000 rpm and 4°C, the precleared supernatant was incubated with protein G-Sepharose beads and control IgG (300 μl) or specific antibodies (1.5 μg for anti-*myc*, 100 μl for anti-A36 and anti-B5, and 5 μl for anti-A33) overnight for 1 h at 4°C while being mixed end-over-end in a tube rotator. After centrifugation for 1 min at 13,000 rpm and 4°C, the supernatant was removed and immunoprecipitates bound to protein G-Sepharose beads were washed extensively with lysis buffer. Finally, the immunoprecipitates were resuspended in denaturant buffer, boiled for 5 min at 95°C, and resolved by SDS-PAGE.

RESULTS

Expression of IEV envelope proteins in transfected cells. The coding sequences of the A33R, A34R, A36R, B5R, F12L, and F13L genes, either alone or fused to epitope tags or GFP, were cloned into eukaryotic expression plasmids. Following the transfection of each construct, the distribution of the corresponding proteins was visualized by immunofluorescence microscopy (Fig. 1A). In accord with previous studies, diverse subcellular distributions were obtained for the different pro-

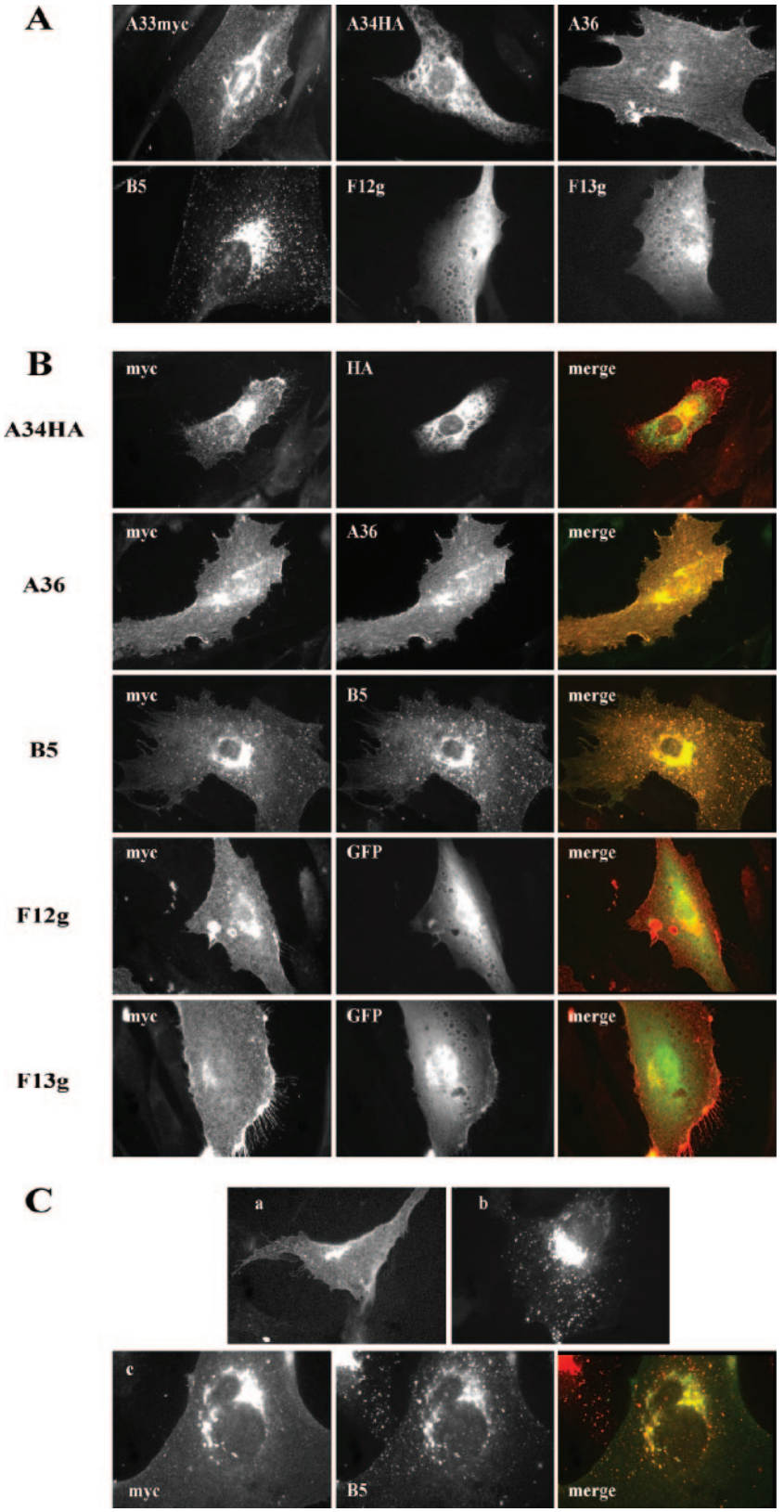

FIG. 1. Interactions of A33 protein with IEV envelope proteins in transfected cells. (A) Intracellular distribution of IEV envelope proteins individually expressed. Immunofluorescence staining was performed on BHK-21 cells transfected with plasmid pcDNA3.1/*myc*-HisB-A33R (A33*myc*), pcDNA 3.1/HA-HisB-A34R (A34HA), pcDNA3.1/A36R (A36), pSG5-B5R (B5), pQBI-F12L (F12g), or pcDNA3.1/p37g (F13g). At 24 h posttransfection, cells were fixed, permeabilized, and directly observed (F12g and F13g) or incubated with the corresponding specific antibodies to *myc*, HA, A36, or B5. Note the diffuse staining pattern of proteins F12 and F13 fused to GFP. (B) Coexpression of A33 with IEV

teins. Protein A33, fused to a *myc* epitope (A33*myc*), was localized to the perinuclear area and to the plasma membrane. Protein A34 fused to the HA epitope (A34HA) produced, in addition to perinuclear staining, a reticulate cytoplasmic pattern. In cells expressing A36, staining was observed in (i) an area in proximity to the nucleus, (ii) the plasma membrane, where staining was more pronounced at the tips of cell projections, and (iii) fibrillar cytoplasmic structures. Protein B5 showed juxtanuclear distribution and a cytoplasmic punctate pattern. F12 protein fused to GFP produced a diffuse cytoplasmic staining. Finally, the fusion protein F13-GFP showed perinuclear staining and diffuse cytoplasmic localization. The intracellular localization of these proteins was in general agreement to that previously reported (5, 15, 19, 21, 35), indicating that the tags used did not have a generalized effect on their distribution. From the above-described results, we concluded that these proteins, except GFP-tagged F12, showed at least some degree of accumulation in areas close to the nucleus (Fig. 1A), which was maximal in the case of B5.

The distribution of A33 when expressed individually by using a Semliki Forest virus replicon has been described previously (21). In those experiments, A33 protein was partially retained in the perinuclear area, although significant amounts reached the cell surface. Transfection experiments with A33*myc*-expressing plasmid produced a similar pattern, indicating that incorporation of the *myc* epitope did not alter the distribution of the protein and confirming that a portion of A33 reaches the plasma membrane.

Coexpression of A33 and IEV envelope proteins in transfected cells. The observation that the individual expression of different IEV proteins produces diverse immunofluorescence patterns makes it possible to detect protein-protein interactions by coexpression of several proteins. With the aim of identifying interactions involving A33, we carried out cotransfection experiments to express A33*myc* together with other virus envelope proteins, followed by immunofluorescence (Fig. 1B). Coexpression of A33 with either A36 or B5 resulted in a high level of colocalization for the two proteins in immunofluorescence images. In contrast, expression of A33 together with A34, F12, or F13 did not result in significant colocalization. These results suggest that direct A33-A36 and A33-B5 interactions take place in transfected cells in the absence of other viral proteins. Of these, A33-A36 interaction has been previously demonstrated and studied in detail (31, 43, 45). In contrast, the A33-B5 interaction has not been detected in previous studies. Colocalization of A33 and B5 was confirmed by the expression of A33*myc* in a cell line constitutively expressing B5 (Fig. 1C).

Construction and characterization of a recombinant vaccinia virus expressing *myc*-tagged A33. To confirm the data obtained from transfection experiments and to further study protein-protein interactions in the context of infection, a recombinant virus (vA33R*myc*) was obtained by inserting the A33R*myc* gene into the A33R deletion mutant. vA33R*myc* is expected to produce a protein of 26 to 31 kDa resulting from the fusion of the A33 protein with the *myc*His_6 epitope. Western blot analysis of vA33R*myc*-infected cells revealed the presence of a protein with the expected electrophoretic mobility that reacted with anti-*myc* antibody (Fig. 2A).

In previous studies, it has been shown that vΔA33R produces normal or elevated amounts of enveloped virions but is unable to induce actin tails and has a tiny plaque phenotype (30). Thus, deletion of A33R does not block virus egress but results in severe effects in virus cell-to-cell transmission. To investigate whether A33*myc* is a functional version of the A33 protein, the phenotype of vA33R*myc* regarding virus transmission and actin tail formation was compared to those of WR and parental virus vΔA33R (Fig. 2B and C). In a standard plaque assay, vA33R*myc* plaques were significantly larger than those of vΔA33R, demonstrating that A33*myc* can provide A33 function. However, vA33R*myc* plaques did not reach the sizes of the plaques formed by the WR virus strain, indicating some effect of introducing the epitope tag (Fig. 2B).

Since the deletion of A33R completely abrogates the ability of vaccinia virus to induce actin tails (30), we also tested the function of A33*myc* in actin tail formation. vA33R*myc*-infected cells were stained with Alexa-phalloidin and observed under a fluorescence microscope (Fig. 2C). In contrast with vΔA33R, vA33R*myc* was able to induce actin tails in infected cells. This result indicates that the A33*myc* fusion protein can functionally replace normal A33 protein.

Coimmunoprecipitation of A33 with IEV envelope proteins. We next searched for interactions between A33*myc* and A36, B5, and F13 by performing coimmunoprecipitation experiments with extracts prepared from infected cells at 24 h postinfection (Fig. 3). Anti-A36 and anti-B5 antibodies immunoprecipitated A33*myc* protein in extracts of vA33R*myc*-infected cells. Also, anti-*myc* antibodies were able to immunoprecipitate F13, although the amount of F13 immunoprecipitated was small compared to the amount present in the cell extract. This may be explained by the stoichiometry and/or the strength of the interaction.

The above-described coimmunoprecipitation experiments suggested the existence of the following interactions between IEV envelope proteins: A33-A36, A33-B5, and A33-F13. In contrast, the existence of an A33-A34 complex could not be

envelope proteins. Immunofluorescence staining was carried out on BHK-21 cells transfected with pcDNA3.1/*myc*-HisB-A33R together with plasmids expressing the proteins indicated on the left. At 24 h posttransfection, cells were fixed, permeabilized, stained with specific antibodies (anti-*myc*, anti-HA-fluorescein, anti-*myc*-FITC, anti-A36, or anti-B5 followed by secondary rabbit anti-mouse IgG-TRITC), observed and photographed under a fluorescence microscope. The merged images result from the combination of the *myc* signal corresponding to A33*myc* and the signal corresponding to the second protein. (C) Distribution of A33 protein after transfection of a cell line stably expressing B5 protein. (a) BHK-21 cells transfected with plasmid pcDNA 3.1/*myc*-HisB-A33R were fixed at 24 h posttransfection, permeabilized, and incubated with anti-*myc*-FITC. (b) BHK-21 cells stably expressing B5 protein (BHK-B5) were fixed, permeabilized, and incubated with anti-B5 followed by anti-mouse-TRITC. (c) BHK-B5 cells transfected with plasmid pcDNA 3.1/*myc*-HisB-A33R were fixed at 24 h posttransfection, permeabilized, and incubated with anti-*myc*-FITC, anti-B5, and anti-mouse-TRITC. Note the colocalization of A33 and B5 signals in the merged image.

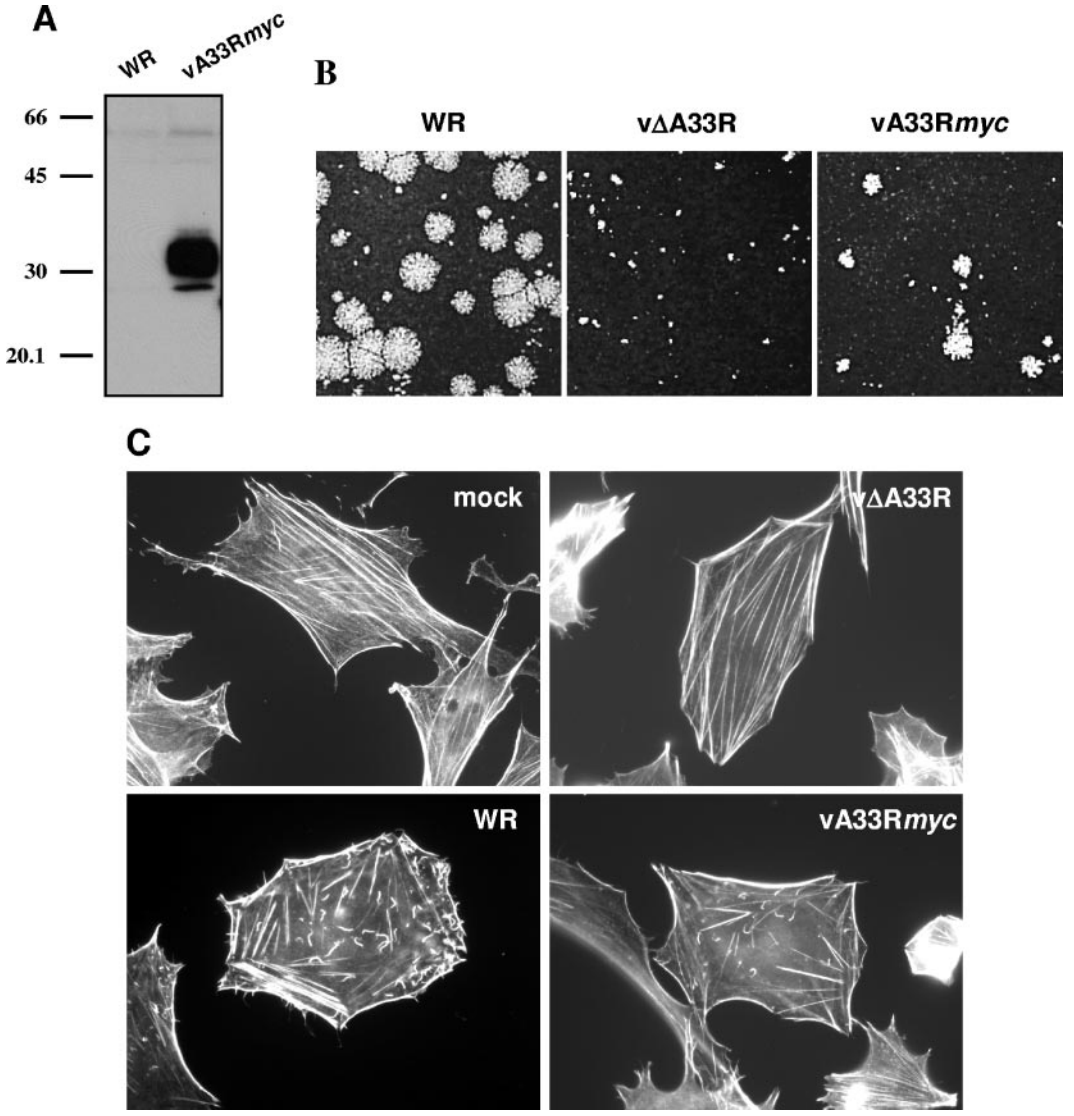

FIG. 2. Characterization of a recombinant vaccinia virus expressing a *myc*-tagged version of the A33 protein. (A) Analysis of A33*myc* expression by Western blotting. Extracts of BSC-1 cells infected with the recombinant vaccinia virus expressing fusion protein A33*myc* (vA33R*myc*) or control virus (WR) were probed with anti-*myc*-HRP antibody. Positions of protein molecular mass markers (in kDa) are indicated. (B) Plaque formation by vA33R*myc*. BSC-1 cell monolayers infected with WR, parental vΔA33R, or vA33R*myc* were incubated for 2 days, stained with crystal violet, and photographed. (C) Induction of actin tails by vA33R*myc*. BHK-21 cells infected for 7 h were fixed, permeabilized, and incubated with 1 unit/ml Alexa594-phalloidin. Note the presence of actin tails in vA33R*myc*-infected cells.

demonstrated (not shown). Among these interactions, A33-A36 was the only one previously described (31). To confirm that the novel interactions of A33 with B5 and F13, observed in the context of an infection with vA33R*myc*, were not due to the epitope tagging of A33, we conducted the coimmunoprecipitation experiments on cell extracts infected with WR by using an antibody to A33 protein (not shown). Thus, the immunoprecipitation experiments indicate that both A33 and A33*myc* interact with B5 and F13.

Targeting of A33 protein to the envelope proteins of mutant viruses. During infection, IEV envelope proteins localize to the Golgi complex or late endosomes, where they are incorporated into infectious viruses that are then transported to the cell periphery and subsequently released into the extracellular medium. Since A33 is necessary for the incorporation of A36 into IEV (45), we sought to determine a similar role for A33 in the intracellular distribution of B5 or F13. We compared the localizations of the B5 and F13 proteins in cells infected with either WR or A33-deficient viruses (Fig. 4). Individual virions were visualized by Hoechst staining and were clearly visible in areas distant from the brightly stained cell nucleus and viral factories. Staining with an antibody to B5 protein in WR-infected cells showed that most B5 in the cell periphery was coincident with the DNA-containing particles, which represent IEV and CEV. The same pattern was detected in vΔA33R-infected cells, indicating that B5 is efficiently targeted to the IEV membrane in the absence of A33 (Fig. 4A).

A staining pattern similar to that of B5 was obtained with

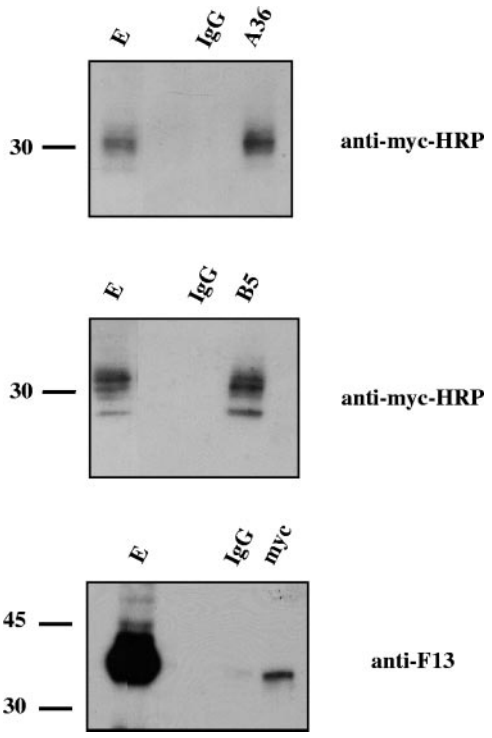

FIG. 3. Coimmunoprecipitation of A33 from infected cells. BSC-1 cells were infected with five PFU per cell of vA33R*myc* and lysed at 24 h postinfection. Immunoprecipitations were performed with either control immunoglobulin G (lanes IgG) or anti-*myc*, anti-A36, or anti-B5 antibodies (indicated at the top of each panel). Western blots were probed with the antibodies indicated on the right side of each panel. E, infected cell extract prior to immunoprecipitation. Immunoprecipitations were performed by use of digitonin-containing buffer, except for the case in which antibody to A36 was used, which was performed using NP-40 as detergent. Molecular-mass markers (in kDa) are indicated.

anti-F13 antibody in WR-infected cells (Fig. 4B), where F13 was detected in peripheral DNA-containing virions. In contrast, F13 distribution was altered in vΔA33R-infected cells, showing predominantly tiny punctate staining that was not restricted to DNA-containing virions. Therefore, the absence of A33 affects the distribution of F13 and results in a defective targeting of F13 into IEV.

Considering the interaction between A33 and B5, we investigated whether B5 was necessary for the incorporation of A33 into IEV. With that aim, we compared the incorporation of *myc*-tagged A33 into enveloped virions in either the presence or the absence of B5. Immunofluorescence on vA33R*myc*-infected cells showed obvious staining of DNA-containing particles in the cell periphery with anti-B5 and anti-*myc* antibodies, confirming that B5 and A33 are enriched in enveloped virions. In congruence with the role of B5 in virus wrapping, the number of virions in the periphery of cells infected with the B5-deficient virus (vA33R*myc*ΔB5R) was greatly diminished. In these cells, A33*myc* showed a diffuse localization and did not colocalize significantly with the few DNA-containing particles (Fig. 4C), pointing to a role for the A33-B5 interaction in the incorporation of A33 into IEV.

The above-described results suggest that B5 is involved in determining the targeting of A33 in the IEV envelope, while A33 has a role in the targeting of F13. In contrast, A33 is not required for incorporation of B5 into IEVs.

Construction and characterization of viruses expressing different versions of B5. To investigate the domain(s) of B5 involved in the interaction with A33, a series of recombinant viruses expressing mutated forms of B5 were constructed. B5 is a 42-kDa type I membrane glycoprotein with a short signal peptide (residues 1 to 19), a large extracellular domain including four SCRs (residues 20 to 236) plus a stalk region (residues 237 to 276), a transmembrane domain (residues 277 to 303), and a short cytoplasmic tail (residues 304 to 317) (9, 16). The different B5 versions constructed were termed according to the domains maintained, R being the short consensus repeats, S the stalk region, T the transmembrane domain, and C the cytoplasmic tail. Thus, RSTC represents the complete B5 protein. Versions deleted in different domains of B5 were constructed (Fig. 5). In addition, and to facilitate detection, the V5 epitope was inserted after the signal peptide sequence so that, after removal of the signal peptide, the V5 epitope is exposed at the N terminus of each mutated protein. The different B5 versions were assembled in plasmids and introduced by recombination into the B5R locus of WRΔB5R.

Since the B5 protein is replaced by the mutated V5-tagged versions, the phenotype of the resulting recombinants should reflect the ability of mutated forms of B5 to provide normal B5 function. Thus, the plaque phenotypes of recombinant viruses were compared with that of WR and their parental WRΔB5R (Fig. 6). Wild-type-sized virus plaques were formed by recombinant virus vRSTC, indicating that the fusion of the V5 epitope to the N terminus of B5 did not affect the functionality of the protein. vRST plaques were also similar in size to WR plaques, indicating that the deletion of the cytoplasmic tail of B5 did not affect virus transmission, in agreement with previous studies (22, 23). In contrast, recombinant virus vTC produced small plaques, similar in size to those of the parental WRΔB5R. However, when the stalk region was included (virus vSTC), the virus made comet-shaped plaques, as reported previously for similar mutations (12). Two virus mutants expressing versions of B5 protein lacking the transmembrane anchor were constructed. vR contained only the SCR domain, and vRS contained both the SCR domain and the stalk region. These two viruses produced small plaques similar to those of WRΔB5R, suggesting that membrane anchoring is essential for B5 function in virus transmission.

An additional version was constructed by replacing the B5 transmembrane domain with that of the VSV G protein. The resulting recombinant virus (vRST$_G$C) produced small plaques that occasionally were slightly larger than those of WRΔB5R. Finally, a B5 version containing a proline-to-serine mutation in position 189 (P189S) was introduced. The P189S mutation was selected because it has been shown to enhance the release of virus into the extracellular medium and to produce a comet-shaped plaque phenotype (17). As expected, the recombinant virus carrying the P189S mutation in B5 (termed vR*STC) produced comet-shaped virus plaques, indicative of increased EEV release.

The above-described recombinant viruses were predicted to produce B5-tagged versions ranging from 9 kDa (version TC) to 37.2 kDa (versions RSTC and R*STC). To test for the

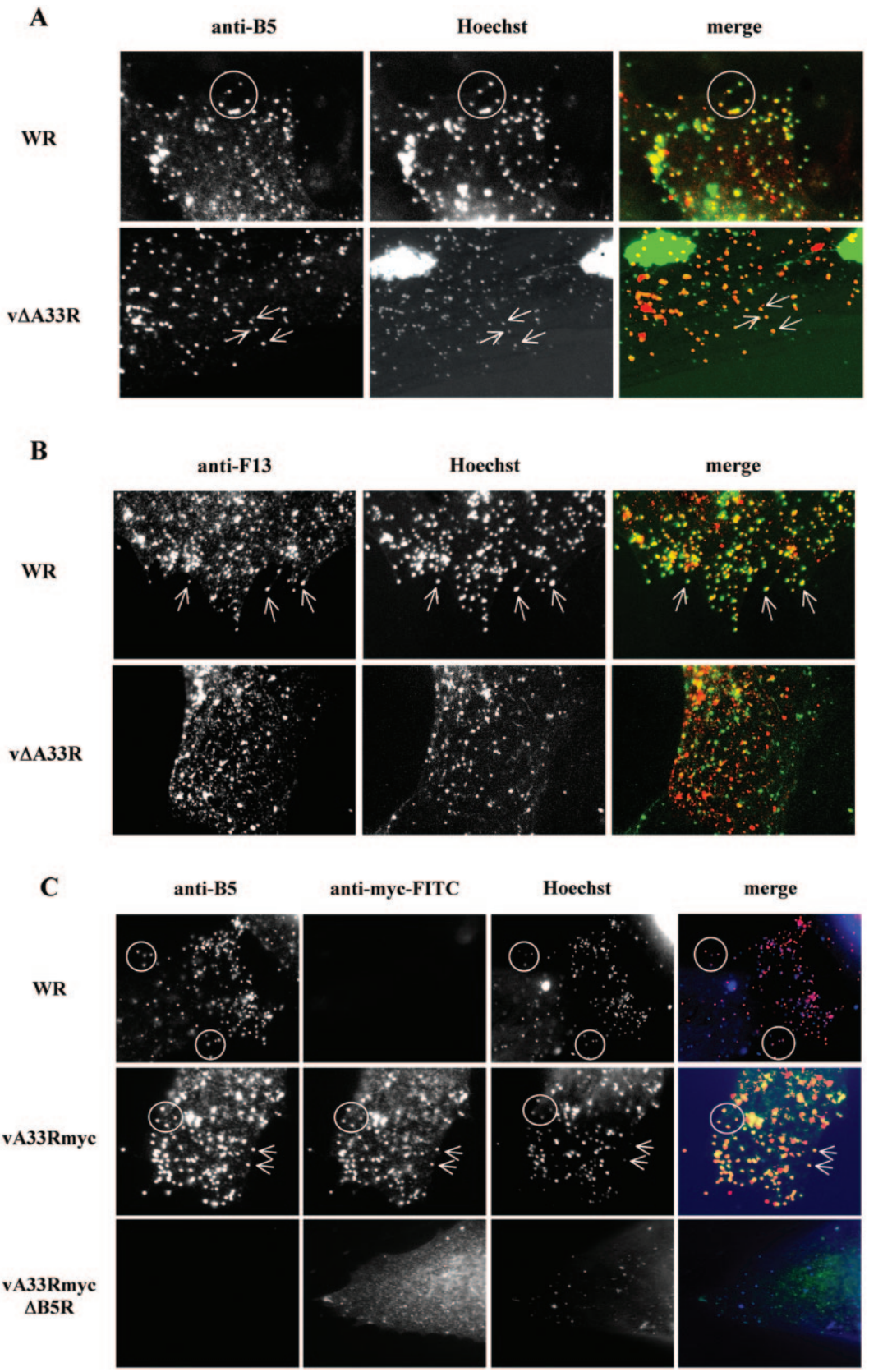

FIG. 4. Distribution of IEV envelope proteins in A33- or B5-deficient viruses. BHK-21 cells were infected for 7 h, fixed, permeabilized, and stained with antibodies against IEV envelope protein A33, B5, or F13. DNA was visualized by Hoechst staining. (A) Colocalization of B5 and virus particles. Cells infected with WR or A33-deficient virus (vΔA33R) were stained with anti-B5 antibody. Merged images result from the combination of monochrome images pseudocolored to red (anti-B5 antibodies) and green (Hoechst). Note the colocalization of B5 protein with viral DNA in cells infected with WR (circles) and vΔA33R (arrows). (B) Colocalization of F13 and virus particles. Cells infected with WR or A33-deficient

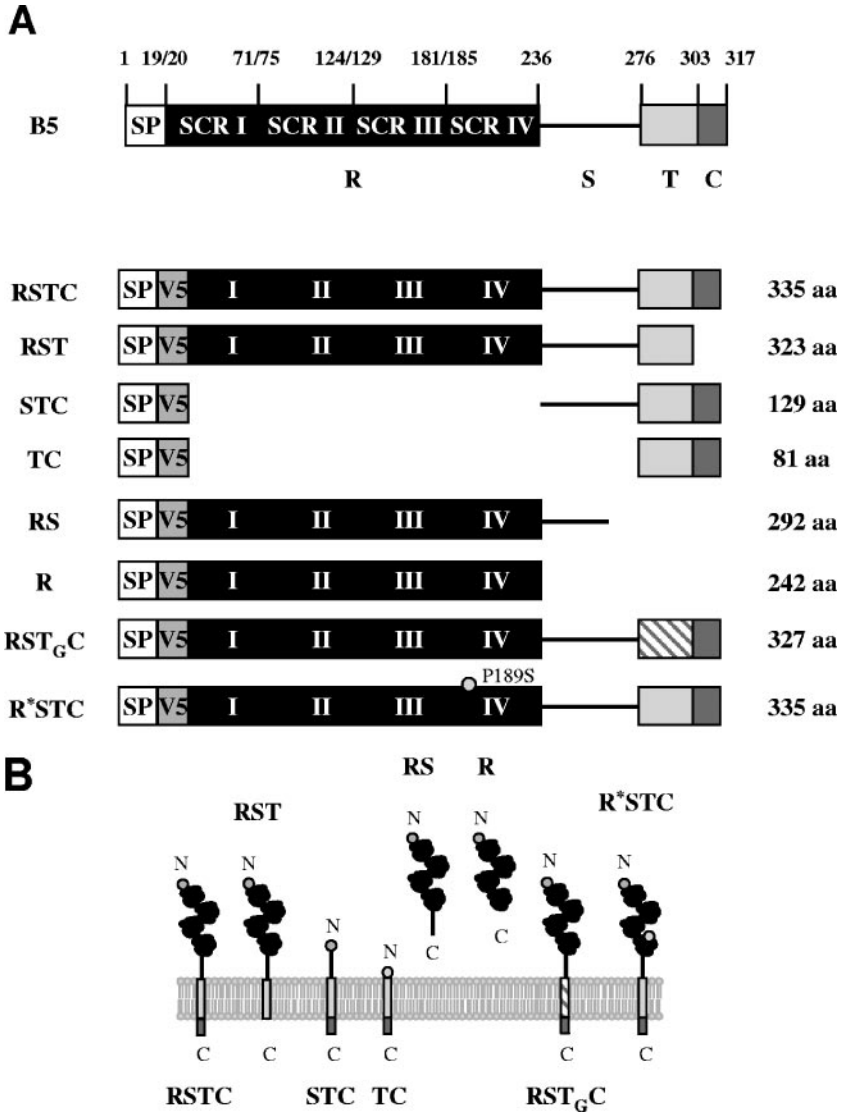

FIG. 5. V5-tagged, mutated versions of the B5 protein. (A) Schematic representation of V5-tagged B5 versions used in this study. SP, signal peptide; V5, V5 epitope; R, four short consensus repeats (SCR I to IV); S, stalk; T, transmembrane domain; C, cytoplasmic tail; aa, amino acids. Versions were termed, as indicated on the left, according to the domains included in the construct. T_G indicates the transmembrane domain of VSV G protein. R* indicates an R region including a P189S mutation located in SCR IV. (B) Predicted topology of mutated B5 versions in the outer membrane of the EEV particle. Domains above the lipid bilayer are in the lumen of the wrapping membranes or the extracellular space, whereas domains below the membrane are cytosolic. The N and C termini are indicated.

correct expression of these, we carried out Western blot analysis of cells infected with the recombinant viruses by using anti-V5 antibody (Fig. 7A). All the versions (except TC) were expressed and reacted with anti-V5 antibody. Version TC was not detected in Western blots (not shown), and therefore, this version was not included in further experiments. Versions RSTC and RST produced, in addition to the B5 monomer, higher-molecular-weight complexes, which might represent homo- or heterodimers. In contrast, these high-molecular-weight protein complexes were absent in vRST$_G$C-infected cell extracts, suggesting that the B5 transmembrane domain is important for the formation of this complex.

virus (vΔA33R) were stained with anti-F13 antibody. Merged images result from the combination of monochrome images pseudocolored to red (anti-F13 antibodies) and green (Hoechst). Note that the colocalization of F13 protein with viral DNA in cells infected with WR (arrows) is affected in vΔA33R-infected cells. (C) Colocalization of A33 and virus particles. Cells infected with WR, vA33R*myc*, or the corresponding B5R deletion mutant vA33R*myc*ΔB5R (indicated on the left) were stained with anti-B5 and anti-*myc* antibodies. Merged images result from the combination of monochrome images pseudocolored to red (anti-B5), green (anti-*myc*), and blue (Hoechst). Note that, in the absence of B5 protein, no colocalization of A33*myc* with viral DNA is observed.

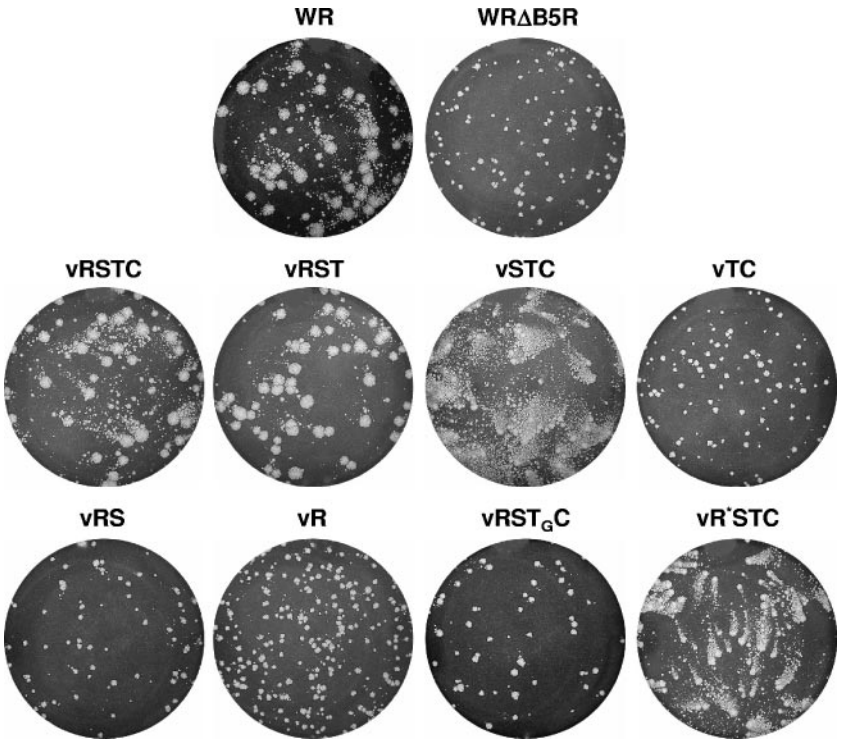

FIG. 6. Plaque phenotypes of recombinant viruses expressing V5-tagged, mutated B5 versions. BSC-1 cell monolayers infected with WR, parental WRΔB5R, or the recombinant viruses indicated were incubated for 2 days, stained with crystal violet, and photographed.

N glycosylation of the V5-tagged versions of B5 was also tested as an indicator of correct expression and transport of the mutated proteins (Fig. 7B). Western blot analysis of cells infected with viruses expressing V5-tagged B5 in the presence or absence of tunicamycin demonstrated that all the versions containing the SCR domain were N glycosylated. In contrast, when the SCR domain was deleted (vSTC), no glycosylation was apparent. This result is in accord with previous reports showing that glycosylated residues lie in the SCR domain of B5 (16).

Finally, we studied the ability of version RS, in which B5 lacks the transmembrane anchor, to be secreted to the extracellular medium. With this aim, supernatants of cells infected with vRS were subjected to Western blot analysis (Fig. 7C). This experiment revealed the presence of a B5 soluble version in the supernatant of vRS-infected cells that was absent in vRSTC-infected cell supernatants. However, the amount of version RS secreted to the medium was small compared to the amount of protein present in the cell lysate.

Localization of V5-tagged, mutated B5 versions by fluorescence microscopy. The intracellular distribution of mutated B5 versions was analyzed by fluorescence microscopy in cells infected with viruses expressing the V5-tagged, mutated B5 versions (Fig. 8). The distribution of full-length B5 (RSTC), as revealed by staining with anti-V5 antibody, reflected the typical B5 distribution, with a strong juxtanuclear signal which corresponds to the Golgi area and peripheral staining of virions. This pattern is termed the EEV envelope pattern (13). The B5 distribution in vRTSC-infected cells, as revealed by anti-V5 staining, was similar to that obtained with WR-infected cells by use of anti-B5 antibody (not shown), providing evidence that the fusion of the V5 epitope to the N terminus of B5 was not affecting B5 distribution. Also, cells infected with viruses vRST, vSTC, and vR*STC showed a normal distribution of B5 protein. Thus, neither the deletion of the cytoplasmic tail (as previously noted [22]), the deletion of the SCR domain, nor the P189S mutation significantly affected B5 distribution.

In contrast, the remaining B5 versions significantly deviated from the envelope pattern. Version RST$_G$C was concentrated in a central area that was more extended than the Golgi area and also showed peripheral punctate staining. Versions RS and R, lacking the transmembrane anchor, labeled an extensive central area and showed a reticulate pattern. These results indicate that proper B5 localization requires the transmembrane domain of B5. This observation was consistent with the plaque phenotype observed since recombinants expressing B5 versions lacking the transmembrane domain produced small virus plaques (Fig. 6).

Mapping the A33-B5 interaction by coimmunoprecipitation experiments. Based on the previous identification of A33-B5 interaction, we sought to determine the B5 domain(s) required for this interaction. Thus, coimmunoprecipitation experiments were performed on extracts prepared from cells infected with the recombinant viruses expressing versions of B5 (Fig. 9). Anti-A33 antibody immunoprecipitated the full-length RSTC version containing the V5 epitope, indicating that the epitope tag was not affecting the interaction with A33. Version RST, lacking the cytoplasmic tail, was also efficiently immunoprecipitated by anti-A33 antibody, indicating that the cytoplasmic tail was not necessary for the interaction of B5 with A33.

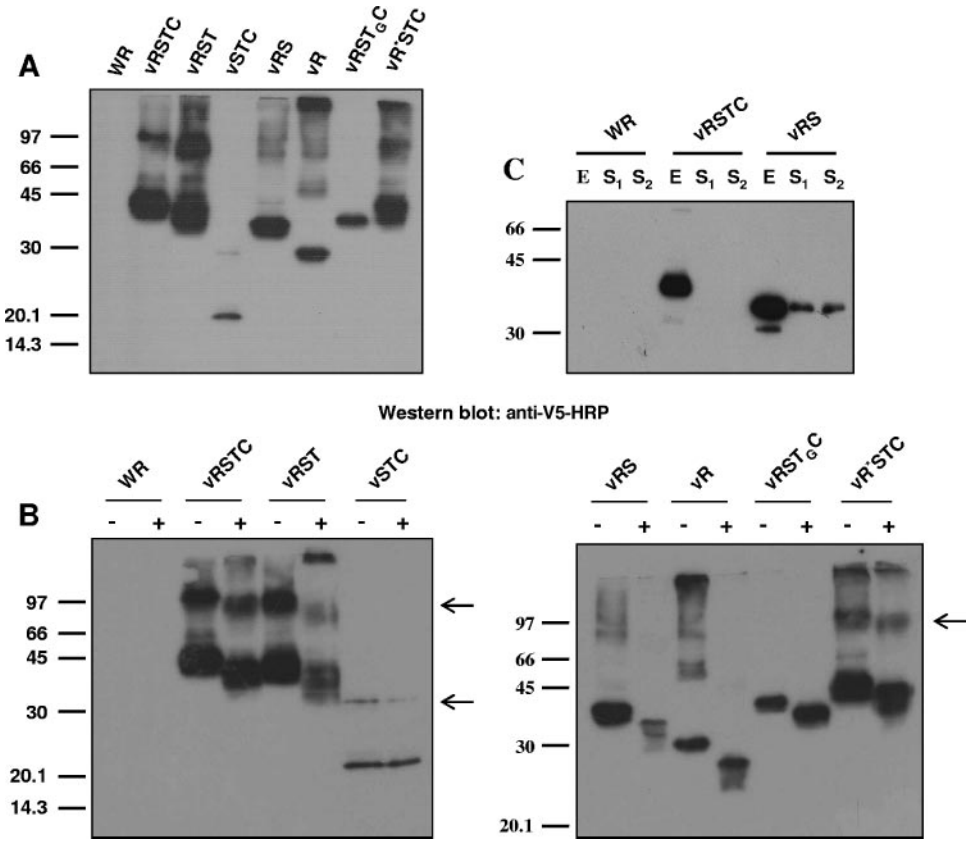

FIG. 7. Characterization of V5-tagged, mutated B5 versions. (A) Western blot analysis. BSC-1 cells were infected with the viruses indicated at the top of the panel at five PFU per cell for 24 h. Western blots were probed with anti-V5-HRP antibody. (B) Analysis of N glycosylation. BSC-1 cells infected with the viruses indicated in the presence (+) or absence (−) of 1 μg/ml tunicamycin were harvested at 24 h postinfection. Western blots were probed with antibody against the V5 epitope conjugated with horseradish peroxidase. Arrowheads point to B5 complexes, which are absent in extracts of cells infected with viruses expressing B5 versions RS, R, and RST_GC. Positions of protein molecular-mass markers are indicated (in kDa). (C) Secretion of B5 soluble version from vRS-infected cells. BSC-1 cells were infected with the viruses indicated at five PFU per cell, harvested at 24 h postinfection, and probed with anti-V5-HRP antibody. E, total cell lysate; S_1, culture medium filtered through 0.1-μm filters (to eliminate vaccinia virus) and concentrated; S_2, culture medium concentrated. Note the presence of the B5 version in the supernatant of vRS-infected cells.

Significantly, version STC, lacking most of the extracellular domain of B5, was also immunoprecipitated. Although the amount of STC immunoprecipitated was small, this probably reflects the small amount of this B5 version present in the cell extracts. In contrast, versions RS and R were not immunoprecipitated. These results point to the transmembrane domain as the portion of B5 critical for mediating the interaction with A33. To preclude the possibility that mere membrane association was the requirement for the interaction to take place, we performed coimmunoprecipitation experiments on $vRST_GC$-infected cell extracts. The results indicate that swapping of the B5 transmembrane domain with that of VSV G protein abrogated the interaction almost completely, suggesting that the transmembrane domain of the B5 protein is the major determinant in the interaction with A33.

It has been previously reported that particular mutations in both B5 and A33 produce an enhanced release of virus into the extracellular medium and a comet-shaped plaque phenotype (17). Specifically, a point mutation (P189S) in the fourth SCR domain of B5 or a C-terminal truncation of 43 amino acid residues in A33 was shown to increase EEV release. We wanted to determine whether this phenotypic effect was related to a loss of the A33-B5 interaction. To investigate this, we introduced these mutated forms in vaccinia virus recombinants and tested for the A33-B5 interaction by immunoprecipitation. The mutated (P189S) B5 protein, expressed by virus vR*STC, was efficiently immunoprecipitated by anti-A33 antibody (Fig. 9). Also, the truncated form of A33, lacking the 43 C-terminal amino acids, was immunoprecipitated by anti-B5 antibody (Perdiguero and Blasco, unpublished). These results demonstrate that the effects of those mutations are not related to changes in the A33-B5 interaction.

DISCUSSION

The presence of multiple proteins in the envelope of vaccinia IEV led us to hypothesize that interactions between those proteins might be influencing their intracellular localization and/or their incorporation into virus particles. To date, several studies have pointed to protein-protein interactions as determinants of the intracellular localization of virus-encoded proteins in the wrapping membranes. For instance, individual ex-

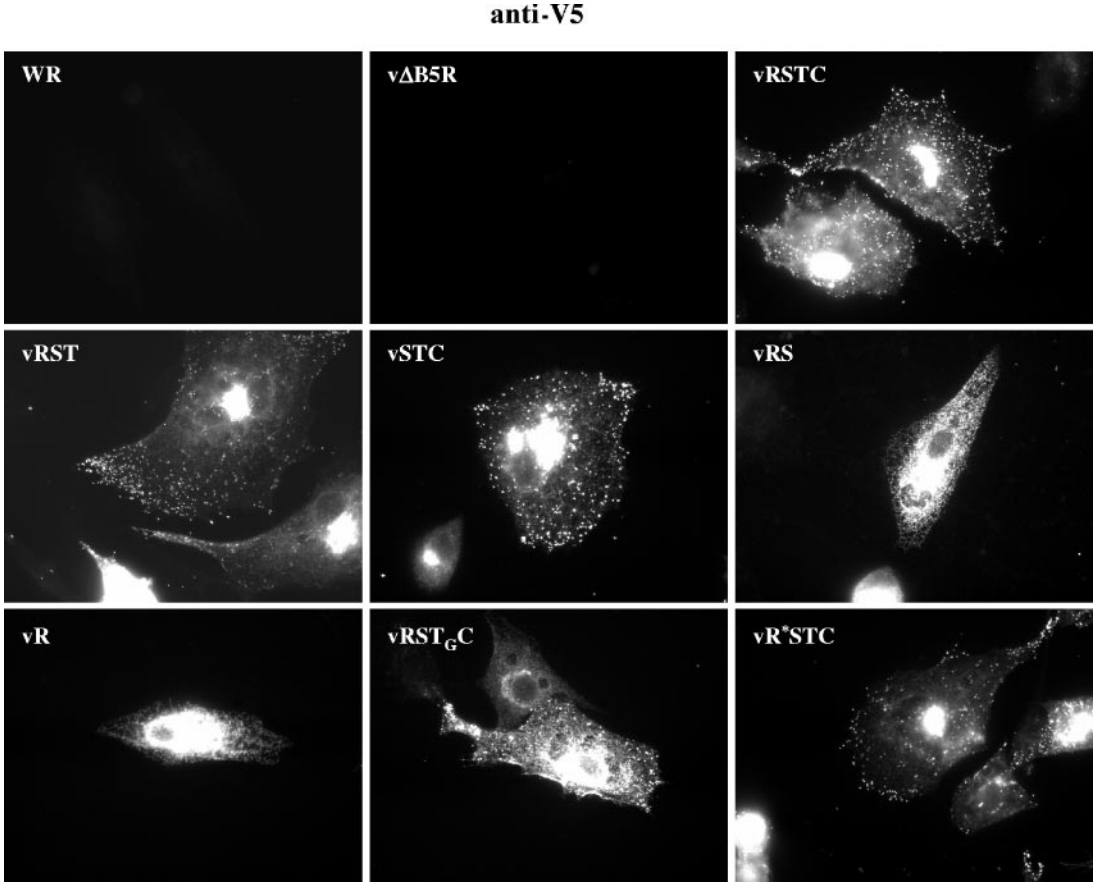

FIG. 8. Intracellular distribution of V5-tagged B5 versions in WR-infected cells. BHK-21 cells infected with the viruses indicated at five PFU per cell were fixed at 7 h postinfection, permeabilized, and labeled with antibody to the V5 epitope followed by secondary rabbit anti-mouse IgG-TRITC to detect the distributions of the different B5 versions.

pression of IEV envelope proteins produces intracellular localization patterns that in general differ from those found in infected cells, suggesting that several virus-encoded proteins cooperate to mediate their enrichment into the wrapping compartment. In addition, several examples of modulation in the distribution of certain IEV envelope proteins have been reported. For instance, the distribution of F13 and its palmitylation are modified by infection (5). Also, the distribution of B5 is modified by coexpression of F13 (15), and the incorporation of A36 into IEV membranes has been shown to depend on the expression of A33 (45).

Our present work focused on the identification of interactions between A33 and other IEV envelope proteins and their functional implications in the morphogenetic pathway of vaccinia virus. Such analysis was carried out in the absence of vaccinia virus infection, by expressing proteins from transfected plasmids, and in the context of virus infection by coimmunoprecipitation experiments with vaccinia virus-infected cells.

The search for interactions established by A33 using transfection experiments was facilitated by the fact that A33, when expressed in transfected cells, is poorly concentrated in the Golgi complex. In previous work from our laboratory (21), where A33 protein was expressed from a Semliki Forest virus replicon, the protein was partially intracellular but was detectable at the plasma membrane, whereas during infection, it was mostly intracellular. To account for this divergence, we sought to identify the protein(s) that modulates the distribution of A33. Following coexpression of A33 and other IEV envelope proteins, colocalization of A33 with A36 or B5 was apparent, suggesting that A33 is capable of associating with A36 or B5 (Fig. 1).

The analysis of protein complexes during virus infection by immunoprecipitation experiments confirmed both A33-A36 and A33-B5 interactions (Fig. 3). Of these, the interaction of A33 with A36 has been characterized in detail (31, 43, 45). In contrast, A33-B5 interaction has not been demonstrated, despite attempts to coimmunoprecipitate A33 and B5 (31). In our hands, the physical association of A33 and B5 in infected cells was confirmed consistently by coimmunoprecipitation experiments. It is likely that the previous attempts failed because of the antibodies or the experimental conditions used.

We questioned whether any of the interactions involving A33 were required for its targeting to the IEV envelopes. Previous studies have not identified any interaction required for incorporating A33 into IEV. In the case of A33-A36, the interaction is needed for the incorporation of A36 but not for that of A33 (45). Hence, the intracellular fate of A33 is not dependent on A36. We therefore investigated a possible role for B5. Our finding that A33 is not targeted efficiently into IEV

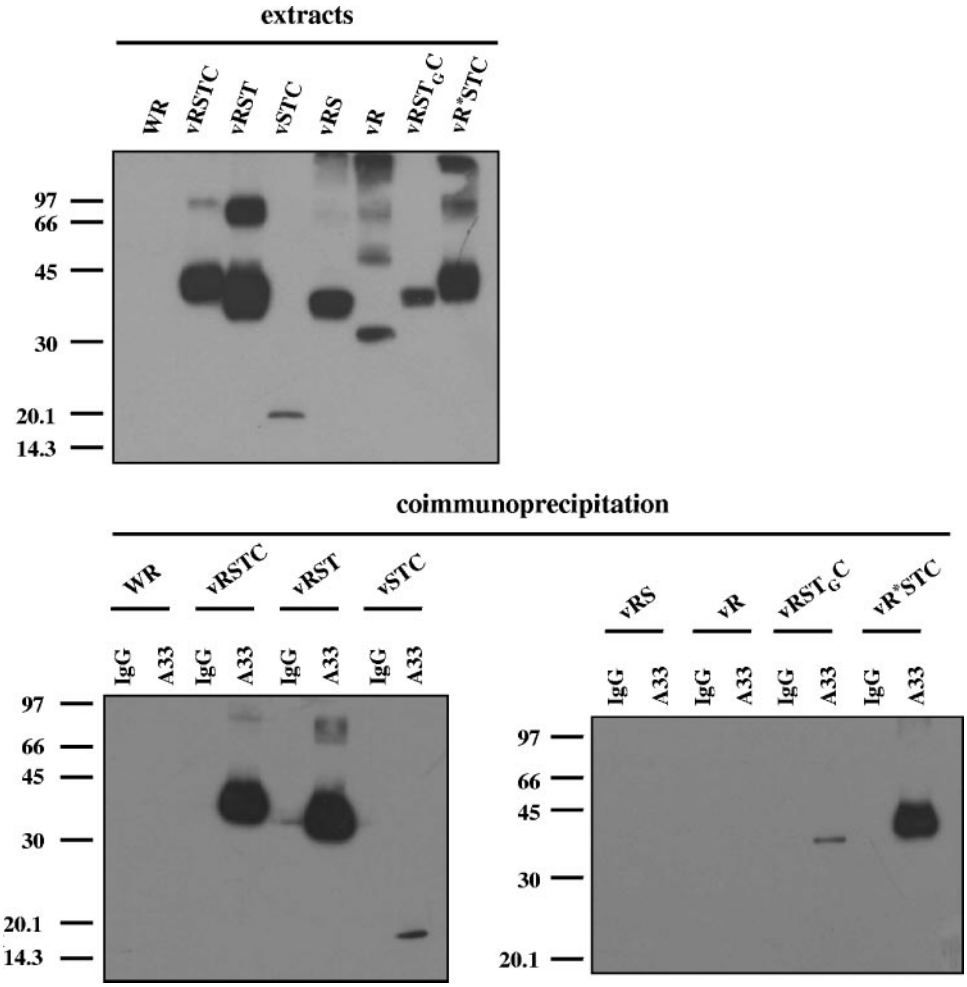

FIG. 9. Mapping of the A33-B5 interaction site by coimmunoprecipitation. BSC-1 cells were infected with the viruses indicated above the panels at five PFU per cell and harvested at 24 h postinfection. The top panel shows infected cell extracts prior to immunoprecipitation, probed with anti-V5 antibody conjugated with horseradish peroxidase. Immunoprecipitations were performed with either control immunoglobulin G (lanes IgG) or anti-A33 antibody (lanes A33), as indicated above the lower panels. Immunoprecipitated material was resolved by SDS-PAGE and subjected to Western blot analysis with anti-V5 antibody conjugated with horseradish peroxidase. Molecular-mass markers are indicated (in kDa).

membranes in B5-deficient virus is consistent with a role for the A33-B5 interaction in the enrichment of A33 in the wrapping membranes.

It seems likely that determining the protein composition of the EEV/CEV envelope relies on multiple protein-protein interactions. Rottger et al. have shown that the distribution of A33 is altered in the absence of A34 (31), although no direct interaction between A33 and A34 has been demonstrated. Interestingly, A34 and B5 have been reported to form a complex (31). In addition, we have found that the incorporation of B5 into IEV is dependent on expression of A34 (Lorenzo, Perdiguero, and Blasco, unpublished results). Thus, the effect of A34R deletion on the distribution of A33 could be mediated by B5. Taking into account all the data, it is possible that the four proteins form a complex, A34-B5-A33-A36. However, since such a large complex has not been detected to date, an alternative possibility is that a diversity of protein complexes involving different combinations of proteins are formed.

The possible role of the A33-B5 interaction in the establishment or modulation of the events leading to virus transport remains to be further investigated. Our results point to a role for protein B5 in incorporating A33, which, in turn, is required for incorporation of A36. Protein A36 is a key player in both the transport of IEV and the induction of actin tails. It has been shown that A36 interacts with kinesin and that this interaction is mutually exclusive with the A33-A36 interaction (42). A36 is phosphorylated by the cellular tyrosine kinase *src*, an event required to induce actin tails. It has been proposed that induction of actin tails at the cell surface requires an outside-in, B5-dependent signaling event triggered by membrane-bound CEV (25). In addition to mutations in A36 and B5, mutations in A33 also abrogate actin tail formation. Of note, no direct interaction between B5 and A36 has been demonstrated. Since A33 interacts with both A36 and B5, these interactions may provide an explanation for how mutations in the three proteins affect the induction of actin tails.

We have shown that A33-B5 interaction is not affected by certain mutations in the B5 protein. For instance, deletion of the SCR domain or the cytoplasmic tail did not have a significant effect on the complex. Further deletion of the stalk region

resulted in the absence of a detectable protein band by immunoblotting, suggesting that this domain is necessary for the stability of the C-terminal portion of the protein. In addition, the transmembrane domain of B5 is important for the intracellular distribution of the protein. It has been reported that the transmembrane domain of B5 contains a signal for exit from the endoplasmic reticulum (41). In agreement with the importance of the transmembrane domain of B5, we have observed altered subcellular distributions in mutated B5 forms lacking the transmembrane domain or with the VSV G protein transmembrane domain replacing the wild-type transmembrane domain (Fig. 8).

Although we cannot formally exclude the possibility that the intracellular location of mutated forms of B5 lacking the transmembrane domain limits the interactions of the protein, the fact that neither the deletion of the cytoplasmic tail nor the deletion of the SCR domain of B5 abrogates the interaction with A33 indicates that the determinants of the interaction lie within the stalk region or the transmembrane domain of B5. While the possibility of a role for the stalk in the interaction cannot be excluded, our results point to the transmembrane domain as the major determinant for the interaction with A33, since the deletion of the B5 transmembrane domain or replacement with that of VSV G protein affected the formation of the A33-B5 complex.

ACKNOWLEDGMENTS

We thank G. L. Smith, G. H. Cohen, and G. Hiller for the generous gift of antibodies and B. Moss for vaccinia virus mutants vΔB5R and vΔA33R.

This work was supported by contract QLK2-CT2002-01867 from the European Commission and grants BMC2002-03047 and BFU2005-05124 from Dirección General de Investigación, Ministerio de Educación y Ciencia, Spain.

REFERENCES

1. **Blasco, R., and B. Moss.** 1991. Extracellular vaccinia virus formation and cell-to-cell virus transmission are prevented by deletion of the gene encoding the 37,000-dalton outer envelope protein. J. Virol. **65:**5910–5920.
2. **Blasco, R., and B. Moss.** 1992. Role of cell-associated enveloped vaccinia virus in cell-to-cell virus spread. J. Virol. **66:**4170–4179.
3. **Blasco, R., and B. Moss.** 1995. Selection of recombinant vaccinia viruses on the basis of plaque formation. Gene **158:**157–162.
4. **Blasco, R., J. R. Sisler, and B. Moss.** 1993. Dissociation of progeny vaccinia virus from the cell membrane is regulated by a viral envelope glycoprotein: effect of a point mutation in the lectin homology domain of the A34R gene. J. Virol. **67:**3319–3325.
5. **Borrego, B., M. M. Lorenzo, and R. Blasco.** 1999. Complementation of P37 (F13L gene) knock-out in vaccinia virus by a cell line expressing the gene constitutively. J. Gen. Virol. **80:**425–432.
6. **Boulter, E. A., and G. Appleyard.** 1973. Differences between extracellular and intracellular forms of poxvirus and their implications. Prog. Med. Virol. **16:**86–108.
7. **Duncan, S. A., and G. L. Smith.** 1992. Identification and characterization of an extracellular envelope glycoprotein affecting vaccinia virus egress. J. Virol. **66:**1610–1621.
8. **Earl, P. L., and B. Moss.** 1991. Expression of proteins in mammalian cells using vaccinia viral vectors, p. 16.15.1–16.18.10. *In* F. M. Ausubel, R. Brent, R. E. Kingston, D. D. Moore, J. G. Seidman, J. A. Smith, and K. Struhl (ed.), Current protocols in molecular biology, vol. 1. Wiley Interscience, New York, N.Y.
9. **Engelstad, M., S. T. Howard, and G. L. Smith.** 1992. A constitutively expressed vaccinia gene encodes a 42-kDa glycoprotein related to complement control factors that forms part of the extracellular virus envelope. Virology **188:**801–810.
10. **Frischknecht, F., V. Moreau, S. Rottger, S. Gonfloni, I. Reckmann, G. Superti-Furga, and M. Way.** 1999. Actin-based motility of vaccinia virus mimics receptor tyrosine kinase signalling. Nature **401:**926–929.
11. **Geada, M. M., I. Galindo, M. M. Lorenzo, B. Perdiguero, and R. Blasco.** 2001. Movements of vaccinia virus intracellular enveloped virions with GFP tagged to the F13L envelope protein. J. Gen. Virol. **82:**2747–2760.
12. **Herrera, E., M. del Mar Lorenzo, R. Blasco, and S. N. Isaacs.** 1998. Functional analysis of vaccinia virus B5R protein: essential role in virus envelopment is independent of a large portion of the extracellular domain. J. Virol. **72:**294–302.
13. **Hiller, G., H. Eibl, and K. Weber.** 1981. Characterization of intracellular and extracellular vaccinia virus variants: N_1-isonicotinoyl-N_2-3-methyl-4-chlorobenzoylhydrazine interferes with cytoplasmic virus dissemination and release. J. Virol. **39:**903–913.
14. **Hirt, P., G. Hiller, and R. Wittek.** 1986. Localization and fine structure of a vaccinia virus gene encoding an envelope antigen. J. Virol. **58:**757–764.
15. **Husain, M., and B. Moss.** 2001. Vaccinia virus F13L protein with a conserved phospholipase catalytic motif induces colocalization of the B5R envelope glycoprotein in post-Golgi vesicles. J. Virol. **75:**7528–7542.
16. **Isaacs, S. N., E. J. Wolffe, L. G. Payne, and B. Moss.** 1992. Characterization of a vaccinia virus-encoded 42-kilodalton class I membrane glycoprotein component of the extracellular virus envelope. J. Virol. **66:**7217–7224.
17. **Katz, E., B. M. Ward, A. S. Weisberg, and B. Moss.** 2003. Mutations in the vaccinia virus A33R and B5R envelope proteins that enhance release of extracellular virions and eliminate formation of actin-containing microvilli without preventing tyrosine phosphorylation of the A36R protein. J. Virol. **77:**12266–12275.
18. **Katz, E., E. Wolffe, and B. Moss.** 2002. Identification of second-site mutations that enhance release and spread of vaccinia virus. J. Virol. **76:**11637–11644.
19. **Katz, E., E. J. Wolffe, and B. Moss.** 1997. The cytoplasmic and transmembrane domains of the vaccinia virus B5R protein target a chimeric human immunodeficiency virus type 1 glycoprotein to the outer envelope of nascent vaccinia virions. J. Virol. **71:**3178–3187.
20. **Krauss, O., R. Hollinshead, M. Hollinshead, and G. L. Smith.** 2002. An investigation of incorporation of cellular antigens into vaccinia virus particles. J. Gen. Virol. **83:**2347–2359.
21. **Lorenzo, M. M., I. Galindo, G. Griffiths, and R. Blasco.** 2000. Intracellular localization of vaccinia virus extracellular enveloped virus envelope proteins individually expressed using a Semliki Forest virus replicon. J. Virol. **74:**10535–10550.
22. **Lorenzo, M. M., E. Herrera, R. Blasco, and S. N. Isaacs.** 1998. Functional analysis of vaccinia virus B5R protein: role of the cytoplasmic tail. Virology **252:**450–457.
23. **Mathew, E. C., C. M. Sanderson, R. Hollinshead, and G. L. Smith.** 2001. A mutational analysis of the vaccinia virus B5R protein. J. Gen. Virol. **82:**1199–1213.
24. **Moss, B.** 1996. Poxviridae: the viruses and their replication, p. 2637–2671. *In* B. N. Fields, D. M. Knipe, and P. M. Howley (ed.), Fields virology, 3rd ed., vol. 2. Lippincott-Raven Publishers, Philadelphia, Pa.
25. **Newsome, T. P., N. Scaplehorn, and M. Way.** 2004. SRC mediates a switch from microtubule- to actin-based motility of vaccinia virus. Science **306:**124–129.
26. **Parkinson, J. E., and G. L. Smith.** 1994. Vaccinia virus gene A36R encodes a M(r) 43–50 K protein on the surface of extracellular enveloped virus. Virology **204:**376–390.
27. **Payne, L. G.** 1992. Characterization of vaccinia virus glycoproteins by monoclonal antibody precipitation. Virology **187:**251–260.
28. **Payne, L. G.** 1980. Significance of extracellular enveloped virus in the in vitro and in vivo dissemination of vaccinia. J. Gen. Virol. **50:**89–100.
29. **Roper, R. L., L. G. Payne, and B. Moss.** 1996. Extracellular vaccinia virus envelope glycoprotein encoded by the A33R gene. J. Virol. **70:**3753–3762.
30. **Roper, R. L., E. J. Wolffe, A. Weisberg, and B. Moss.** 1998. The envelope protein encoded by the A33R gene is required for formation of actin-containing microvilli and efficient cell-to-cell spread of vaccinia virus. J. Virol. **72:**4192–4204.
31. **Rottger, S., F. Frischknecht, I. Reckmann, G. L. Smith, and M. Way.** 1999. Interactions between vaccinia virus IEV membrane proteins and their roles in IEV assembly and actin tail formation. J. Virol. **73:**2863–2875.
32. **Sanchez-Puig, J. M., and R. Blasco.** 2000. Puromycin resistance (pac) gene as a selectable marker in vaccinia virus. Gene **257:**57–65.
33. **Scaplehorn, N., A. Holmstrom, V. Moreau, F. Frischknecht, I. Reckmann, and M. Way.** 2002. Grb2 and Nck act cooperatively to promote actin-based motility of vaccinia virus. Curr. Biol. **12:**740–745.
34. **Schmelz, M., B. Sodeik, M. Ericsson, E. J. Wolffe, H. Shida, G. Hiller, and G. Griffiths.** 1994. Assembly of vaccinia virus: the second wrapping cisterna is derived from the trans Golgi network. J. Virol. **68:**130–147.
35. **Shida, H.** 1986. Variants of vaccinia virus hemagglutinin altered in intracellular transport. Mol. Cell. Biol. **6:**3734–3745.
36. **Smith, G. L., and A. Vanderplasschen.** 1998. Extracellular enveloped vaccinia virus. Entry, egress, and evasion. Adv. Exp. Med. Biol. **440:**395–414.
37. **Smith, G. L., A. Vanderplasschen, and M. Law.** 2002. The formation and function of extracellular enveloped vaccinia virus. J. Gen. Virol. **83:**2915–2931.

38. **Tooze, J., M. Hollinshead, B. Reis, K. Radsak, and H. Kern.** 1993. Progeny vaccinia and human cytomegalovirus particles utilize early endosomal cisternae for their envelopes. Eur. J. Cell Biol. **60:**163–178.
39. **van Eijl, H., M. Hollinshead, G. Rodger, W. H. Zhang, and G. L. Smith.** 2002. The vaccinia virus F12L protein is associated with intracellular enveloped virus particles and is required for their egress to the cell surface. J. Gen. Virol. **83:**195–207.
40. **van Eijl, H., M. Hollinshead, and G. L. Smith.** 2000. The vaccinia virus A36R protein is a type Ib membrane protein present on intracellular but not extracellular enveloped virus particles. Virology **271:**26–36.
41. **Ward, B. M., and B. Moss.** 2000. Golgi network targeting and plasma membrane internalization signals in vaccinia virus B5R envelope protein. J. Virol. **74:**3771–3780.
42. **Ward, B. M., and B. Moss.** 2004. Vaccinia virus A36R membrane protein provides a direct link between intracellular enveloped virions and the microtubule motor kinesin. J. Virol. **78:**2486–2493.
43. **Ward, B. M., A. S. Weisberg, and B. Moss.** 2003. Mapping and functional analysis of interaction sites within the cytoplasmic domains of the vaccinia virus A33R and A36R envelope proteins. J. Virol. **77:**4113–4126.
44. **Wolffe, E. J., S. N. Isaacs, and B. Moss.** 1993. Deletion of the vaccinia virus B5R gene encoding a 42-kilodalton membrane glycoprotein inhibits extracellular virus envelope formation and dissemination. J. Virol. **67:**4732–4741. (Erratum, **67:**5709–5711.)
45. **Wolffe, E. J., A. S. Weisberg, and B. Moss.** 2001. The vaccinia virus A33R protein provides a chaperone function for viral membrane localization and tyrosine phosphorylation of the A36R protein. J. Virol. **75:**303–310.
46. **Zhang, W. H., D. Wilcock, and G. L. Smith.** 2000. Vaccinia virus F12L protein is required for actin tail formation, normal plaque size, and virulence. J. Virol. **74:**11654–11662.